

# A Simple and Effective Extrinsic Calibration Method of a Camera and a Single Line Scanning Lidar

Heng Yang<sup>1\*</sup>, Xiaolin Liu<sup>2</sup>, Ioannis Patras<sup>1</sup>

<sup>1</sup>Queen Mary University of London  
{heng.yang,i.pstras}@eecs.qmul.ac.uk

<sup>2</sup>National University of Defense Technology  
lxl06@yahoo.com.cn

## Abstract

*In this paper we propose an extrinsic calibration method of regular camera and single line scanning lidar which are widely utilized together. Based on a long ignored aspect that infra-red (IR) source for commonly used lidars lies in the response range of regular cameras, we employ an auxiliary IR filter (blocking natural light and letting IR pass) in order for camera to image the scan traces of lidar by prolonging exposure time. Then by scanning V-shaped target such as the intersection of two smooth walls, corresponding lines (or points) on scan plane and image are found through line fitting. With these high confident correspondences, extrinsic parameters (known camera) or a planar homography (unknown camera) can easily be calculated. Furthermore, two evaluation methods, namely line alignment error and two-view point alignment error, are developed. Experiments show that our method greatly simplifies the calibration procedure and outperforms the state-of-the-art in accuracy by using only one-tenth of the calibration data.*

## 1. Introduction

Line scanning lidars, like those from the SICK-LMS family, are capable of providing highly accurate range measurements in large angular fields in real-time. They have several applications together with vision sensors in the areas of robotics and navigation of unmanned ground vehicle in outdoor environments like [3, 4, 5] because these sensors provide complementary information. Fusion of range and visual data requires accurate extrinsic calibration of the sensors. To find transformation of two sensors, several approaches have been proposed. Since lidar source light was mistaken to be in-

visible to regular cameras, the previous methods differ mainly in the way of finding correspondences of the two sensors, explicitly or implicitly.

In explicit category, [5] conducted the calibration by using a solar cell connected to an earphone for scan peak detection. A similar compound device, a tip on a card board was utilized in [7]. These two methods introduced alien sensors to detect scan peaks and let the alien sensors visible to camera. However, the localization of the peak, neither through solar cell nor tip, is accurate enough.

Among implicit methods, Zhang *et al.* [9] proposed using constraints between “views” of a planar chessboard calibration patterns from the camera and lidar based the fact that traditional camera calibration method can extract the normal of the plane. Specific calibration assistant targets were used in [1, 4]. [6] studied the calibration between a central catadioptric camera and a laser range finder based on [9]. Recently Kwak *et al.* [3] also employ a V-shaped target to generate implicit correspondences and have demonstrated the best precise calibration performance up to date. But these methods have three common drawbacks: first, calibration accuracy depends on manufacturing level of assistant targets which generally have high requirement such as [4]; second, since direct correspondences are unavailable, the computation process is complex [3]; third, a large number of data pairs are necessary for optimization, e.g. 100-300 scan/image pairs were used in [3] and each pair required time-consuming manual feature selection.

Our method aims to greatly simplify calibration procedure and improve the accuracy. Our method directly makes laser scan trace (a line made of a sequence of scanning dots) visible to the camera by employing an IR filter. By scanning a V-shaped target such as the intersection of two walls, scanning lines (on planar scene object) and their IR image can be extracted. Once these correspondences are established with high level of confidence, calibration is cast as a perspective-n-point

---

\* The work was mainly done when the author was with NUDT and partly supported by Innovation Fund Grant S100303.

( $PnP$ ) problem for calibrated camera or a planar homography problem for un-calibrated camera. Two quantitative evaluation methods are improved in this paper in order to compare performance in calibration experiments.

## 2. Problem Formulation

### 2.1 Camera-Lidar System

The lidar-camera system model is shown in Fig. 1.  $O_L - X_L Y_L Z_L$  represents the lidar coordinate system with original point at IR emission point and the entire scanning points lie on  $Z_L = 0$  plane.  $O_C - X_C Y_C Z_C$  is camera coordinate system. Scan point and its image are represented as  $P$  and  $p$ .  $(R, t)$  denotes transformation (unknown) from  $O_L - X_L Y_L Z_L$  to  $O_C - X_C Y_C Z_C$ , i.e. extrinsic parameters,  $R$  a 3 by 3 orthonormal matrix representing rotation, and  $t$  a 3-vector representing translation. According to the pinhole camera model, a projection from lidar coordinate  $P = (X, Y, Z)^T$  to the image coordinate  $p = (x, y)^T$  can be represented as follows [2]:

$$s \begin{bmatrix} p \\ 1 \end{bmatrix} = K \left( \begin{bmatrix} R & t \\ \vec{0} & 1 \end{bmatrix} \begin{bmatrix} P \\ 1 \end{bmatrix} \right) \quad (1)$$

where  $s$  is a scale factor and  $K$  is a  $3 \times 3$  camera intrinsic matrix.

### 2.2 Plane to Image Homography

The scanning points of the lidar only lie in a slice of 3D space, according to our defined coordinate, the plane of  $Z = 0$ . Then the mapping from the laser scanning points to their image is a planar projective transformation, or called plane-to-image homography, which is a linear transformation on 3-vector, i.e.

$$s \begin{bmatrix} x \\ y \\ 1 \end{bmatrix} = \begin{bmatrix} h_{11} & h_{12} & h_{13} \\ h_{21} & h_{22} & h_{23} \\ h_{31} & h_{32} & h_{33} \end{bmatrix} \begin{bmatrix} X \\ Y \\ 1 \end{bmatrix} \quad (2)$$

or briefly  $sp' = HP'$ .  $H$  is a non-singular 3 matrix with 8 degrees of freedom which can be defined meaningfully up to an arbitrary non-zero scale factor  $s$ . Since each point correspondence provides 2 equations, 4 exact correspondences (no 3 can be collinear) are sufficient to solve  $H$  by DLT algorithm [2]. Let  $L$  and  $l$  be respectively the scanning line (on planar scene object) and its corresponding image line, according to the duality principle, we also have

$$sL = H^T l. \quad (3)$$

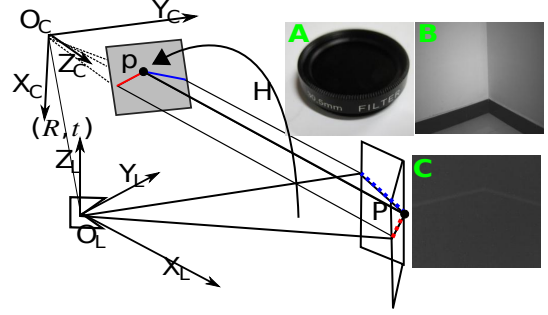


Figure 1. Lidar-camera system and images without (B) and with (C) IR filter (A)

Obviously, from equations(1) (2) and (3), once the correspondences, points or lines are available, we can explicitly solve the parameters of  $(R, t)$  (given  $K$ ) or  $H$  (without  $K$ ). In the following section, we will demonstrate our approach of acquiring the correspondences and the solution based on the correspondences.

## 3 Calibration Procedure

In this section, we summarize our method in 5 steps including the experiment setup (step1,step2), data processing (step3,step4) and pose optimization (step5).

### Step1 Make Range Scanning Trace Visible to Camera:

By investigation of different types of lidars, it is found that the most common form of single line scanning lidars for consumers are laser class 1 devices, conforming the eye-safety requirement, e.g. the most commonly used SICK-LMS family line scanning lidars in application areas of [3, 4, 7, 9, 5] utilize IR light of 905nm wavelength. IR light is invisible to human eyes but visible to regular cameras. Human eyes respond to wavelengths in the range 400 to 700nm whereas a CCD typically responds from 200 to 1100nm. That is to say, 905nm IR light lies in the range of CCD spectral response (or called Quantum Efficiency, QE). However, directly we cannot discover the image of laser scanning traces because the relative QE of IR is lower than that of natural light (Fig. 1(B)). We employ an auxiliary IR filter (Fig. 1(A)) to block the natural light and prolong the exposure time in order to image the scanning trace of the lidar (IR image). After filtering, IR image (Fig. 1(C)) of scan traces are lines made of a sequence of individual scan dots with small gap when lidar keeps continuously scanning.

### Step2 Calibration Data Collection:

Platform is moved around but kept facing the intersection of two smooth walls at arbitrary position so as to acquire IR image like Fig. 1(C). We record  $n$  pairs of range scans and IR im-

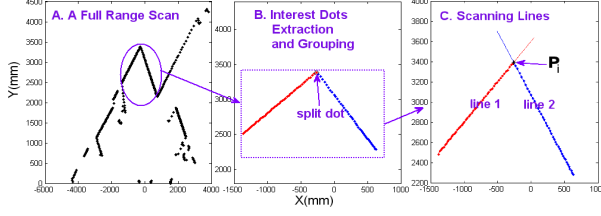


Figure 2. Range data processing

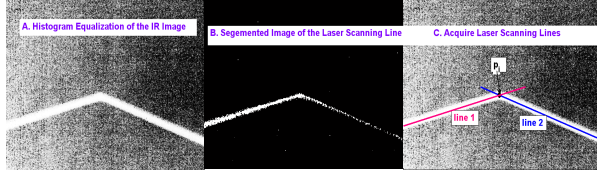


Figure 3. IR image processing procedure

ages at different positions.

**Step3 Range Data Processing:** The process of range data processing is illustrated in Fig. 2. Firstly, scanning points reflected from the two walls are segmented and then a split point is identified so as to group the points into two sets. After that, line fitting is carried out to find two lines  $L_{2i}, L_{2i+1}$  and their intersection  $P_i$  in the scanning plan. We employ this fitting step to greatly decrease the noise and errors instead of depending on the manufacturing level of calibration patterns as previous methods. Furthermore, this fitting procedure also is capable of suppressing the system error of the lidar as we depend on the fitting result instead of any individual scan point.

**Step4 IR Image Processing:** The processing of IR image is illustrated in Fig. 3. Histogram equalization is performed on IR images and flowing with smooth operation as in Fig. 3(A). Then proper threshold is set to segment the scanning trace. When the trace band appears wide in image (very close to the wall), thinning operation is necessary to segment the skeleton of the trace band, shown in Fig. 3(B). At last, Hough Transform (HT) is applied and we obtain two lines as in Fig. 3(C), i.e.  $l_{2i}, l_{2i+1}$  and their intersection is  $p_i$ . This is the only step there might be processing error. We investigate that the widest IR trace is  $\leq 8$  pixels which means even the worst case of thinning and HT could result in no bigger error than 4 pixels. We have carried out simulation experiments and proved that the relative calibration error ( $\frac{\text{error}}{\text{actual value}}$ ) resulted from this level of noise is less than 1%.

**Step5 Computation and Optimization:** From above steps, we now have  $n$  pairs of corresponding points  $\{P_i \leftrightarrow p_i\}$  or  $2n$  pairs of corresponding lines  $\{L_i \leftrightarrow$

$l_i\}$ . When the camera intrinsic matrix  $K$  is available, to solve  $R$  and  $t$  can be formulized into a standard  $PnP$  problem with sound solutions and we simply solve it using Levenberg-Marquardt optimization by minimizing the re-projection error function:

$$\begin{cases} \min_{R,t} \frac{1}{2} \sum_i^n \|f(R, t, P_i, p_i)\|^2 \\ f(R, t, P_i, p_i) = sK(RP_i + t) - p_i \end{cases} \quad (4)$$

When camera intrinsic parameters are unknown, we can compute the planar homography  $H$ . But the error is very huge by directly using DLT algorithm because of the different orders of magnitude of correspondences. Therefore, we apply *normalization* first. The point normalization approach is discussed in [2] and the main idea is to transform the points into a new coordinate such that the centroid of the points is the coordinate origin and their average distance from the origin is  $\sqrt{2}$ . Similar line normalization approach was proposed in [8]. Afterwards, the normalization-based DLT algorithm is carried out for computing scan plane to image homography.

## 4 Experiments

In calibration experiments, SICK LMS-291-05 lidar and regular CCD camera are mounted on a robot platform. The lidar has a  $180^\circ$  horizontal field of view with 75 Hz scanning frequency and we set the measurement resolution 1mm and angular resolution  $0.5^\circ$ . In order to effectively collect the calibration data, we firstly equally divide the image into  $4 \times 4$  subwindows and then move the platform to arbitrary positions, guaranteeing there are two intersection points (like  $p_i$  in 3) in each subwindow. Therefore, we have 32 scan/image pairs with equal distribution in the whole view of camera. The number is much fewer than that in [3]. To demonstrate the performance, we also improved the evaluation methods in [3] and [4] so as to make the comparison reasonably and quantitatively.

### 4.1 Line Alignment Error

As in [3], the line alignment error is the RMS distance between the lidar scan points projected onto the image and the ground truth line. The ground truth line in [3] is from a manually setted colored tape according to scan lines seen through an auxiliary IR camera. In this procedure, large error is unavoidable in both the manual marking and center line extracting. Once again due to convenient availability of scanning line on image, we directly project the corresponding lidar

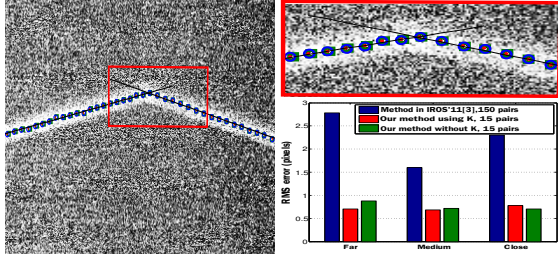


Figure 4. Line alignment error

range data onto the ground truth image using the calibration parameters and compute the line alignment error. The comparison is shown in Fig. 4. Red dots, green rectangles and blue circles are respectively the projection from result of our method with camera parameters, our method without camera parameters and Kwak’s method. In our method, only 15 scan/image pairs are sufficient to achieve better result (line alignment error  $< 1$  pixel ) than state-of-the-art method [3] where hundreds of pairs are required.

#### 4.2 Two-View Point Alignment Error

Inspired by the evaluation idea of [4], we devise a quantitative evaluation method of the two view point alignment based on plane deduced homography. Firstly two cameras are calibrated w.r.t the same lidar. According to calibration parameters, we project the lidar scan points from a chessboard onto two images, as shown in Fig. 5, *A* and *B*. Meanwhile, with the chesscorner correspondences, we compute the plane-deduced homography between the two images,  $H_B^A$ , which maps the position of points (red dots) from *A* to *B* (red circles). And then we compute the RMS distance between the points (red circles and green dots) as point alignment error, or we can call it scene point bias from two views. We put the chessboard at various distance from 2m to 6m with different orientations and the averaged RMS over orientation is shown in Fig. 5. Though 15 scan/image pairs of data are used by our method while 150 pairs of data are used in Kwak’s method, the scene bias of our method is less than that of [3].

In our proposed method, image data corresponds directly to the laser scanning dots, therefore minimizing potential sources of error. On the contrary, algorithm described in [3] has more processing steps, namely in what concerns the correspondences, thereby introducing additional sources of error. Our method has demonstrated significant improvement in calibration accuracy from the above comparison.

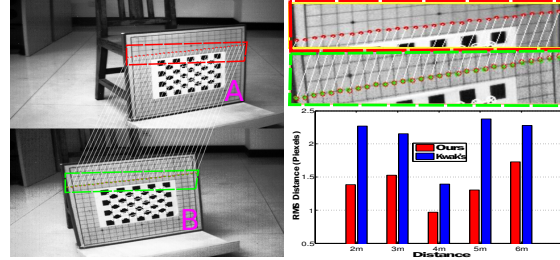


Figure 5. Two-view point alignment error

## 5 Conclusion

In this paper, we have proposed an extrinsic calibration methodology for camera and line scanning lidar based on directly recovering the laser scanning traces in images with the help of IR filter. In this way, line or point correspondences between camera and lidar can be established with high level of confidence. Then we formulate the calibration into a *PnP* problem (known camera) or a planar homography problem (unknown camera). In spite of the fact that only one-tenth of scan/image pairs of data are used for calibration, our method yields significant better result than the state-of-the-art, even under the condition that camera intrinsic parameters are unavailable.

## References

- [1] M. Antone and Y. Friedman. Fully automated laser range calibration. In *BMVC 2007*.
- [2] R. I. Hartley and A. Zisserman. *Multiple View Geometry in Computer Vision*. Cambridge University Press.
- [3] K. Kwak, D. Huber, H. Badino, and T. Kanade. Extrinsic calibration of a single line scanning lidar and a camera. In *IROS 2011*.
- [4] G. Li, Y. Liu, L. Dong, X. Cai, and D. Zhou. An algorithm for extrinsic parameters calibration of a camera and a laser range finder using line features. In *IROS 2007*.
- [5] M. Magai. Calibration methodology for laser scanner external parameters. In *ACRS 2004*.
- [6] C. Mei and P. Rives. Calibration between a central catadioptric camera and a laser range finder for robotic applications. In *ICRA 2006*.
- [7] F. Schweiger, I. Bauermann, and E. Steinbach. Joint calibration of a camera triplet and a laser rangefinder. In *ICME 2008*.
- [8] H. Zeng, X. Deng, and Z. Hu. A new normalized method on line-based homography estimation. *Pattern Recognition Letters*, 2008.
- [9] Q. Zhang and R. Pless. Extrinsic calibration of a camera and laser range finder (improves camera calibration). In *IROS 2004*.